

## Charge-Transfer Efficiency of WFPC2

BRADLEY WHITMORE,<sup>1</sup> INGE HEYER,<sup>2</sup> AND STEFANO CASERTANO<sup>3</sup>

Space Telescope Science Institute, Baltimore, MD 21218

Received 1999 May 27; accepted 1999 September 7

**ABSTRACT.** Observations of  $\omega$  Centauri have been used to characterize the charge-transfer efficiency (CTE) of the Wide Field and Planetary Camera 2 (WFPC2) on board the *Hubble Space Telescope*. A set of formulae has been developed to correct aperture photometry for CTE loss with dependencies on the  $X$ - and  $Y$ -positions, the background counts, the brightness of the star, and the time of the observation. The observations indicate that for very faint stars on a very faint background, the CTE loss from the top to the bottom of a chip has increased from about 3% shortly after the cooldown of WFPC2 (1994 April 23) to roughly 40% in 1999 February. In general, typical WFPC2 exposures are much longer than these short-calibration images, resulting in higher background which significantly reduces the CTE loss and minimizes the CTE problem for most science exposures.

### 1. INTRODUCTION

The advent of charge-coupled device (CCD) technology revolutionized imaging astronomy roughly 20 years ago as a result of the combination of high quantum efficiency and nearly linear response over a large dynamic range ( $\approx 10^5$ ). The ability to transfer a packet of electrons from pixel to pixel with nearly perfect efficiency is critical to the design of CCDs. However, nothing is perfect, and one of the few shortcomings of CCDs is the fact that the efficiency of transferring charge is typically  $\sim 0.99995$  rather than 1.0000. The observational consequence of nonoptimal CTE is that a point source observed at the top of the chip appears to be fainter than if observed at the bottom of the chip, since more of the charge gets “trapped” during the readout for the stars near the top of the chip. By convention, the direction of the readout down the chip is the  $Y$ -axis (or parallel axis), while the  $X$ -axis (or serial axis) is the direction of the readout of the shift register at the bottom of the chip.

During the first year after launch the standard solution for correcting for CTE loss in the  $Y$ -direction (referred to as  $Y$ -CTE loss or simply CTE loss in this paper; often also referred to as parallel CTE loss in the literature) for the Wide Field and Planetary Camera 2 (WFPC2) was to use a 4% linear ramp in cases with low background and no correction for cases with high background (Holtzman et al. 1995). On-orbit data has provided a more detailed characterization (Whitmore & Heyer 1997, hereafter Paper I) with

dependencies on the  $X$ - and  $Y$ -positions, background counts, and target background. In addition, a temporal dependence was reported in Whitmore (1998, hereafter Paper II).<sup>4</sup> The current paper provides a summary of these two papers, plus an update based on data obtained in 1998 and 1999 February. The latest observations indicate that CTE loss can be as much as 40% from top to bottom of the chip for very faint stars on very faint backgrounds. Very extended sources (e.g., flat fields) show little or no CTE loss.

The apparent cause of the increase in CTE loss based on recent laboratory tests is radiation damage (Janesick et al. 1991). This is particularly important for spaceborne CCDs such as the WFPC2 where the levels of radiation are significantly higher. The problem is especially critical for large format CCDs such as the Advanced Camera for Surveys (ACS), and the Wide Field Camera 3 (WFC3), both scheduled for the *Hubble Space Telescope*. These have more than 2.5 times the number of pixels to traverse during the readout.

An independent measurement of CTE has been made by Stetson (1998) by comparing WFPC2 observations with ground-based observations of  $\omega$  Centauri and NGC 2419. In general, the results are quite similar to the those reported in Papers I and II. However, while he confirms the dependencies on the  $X$ - and  $Y$ -coordinates, target brightness, and background level, he also finds a substantially smaller temporal dependence than reported in Paper II or the current

<sup>1</sup> whitmore@stsci.edu.

<sup>2</sup> heyer@stsci.edu.

<sup>3</sup> stefano@stsci.edu.

<sup>4</sup> B. C. Whitmore, Time Dependence of the Charge Transfer Efficiency, is available on-line at [http://www.stsci.edu/instruments/wfpc2/wfpc2\\_doc.html#Stat](http://www.stsci.edu/instruments/wfpc2/wfpc2_doc.html#Stat).

TABLE 1  
DATA SETS USED IN THE ANALYSIS

Date	MJD	Gain	Exposure (s)	Data Set(s)	Filter	Background (DN) <sup>a</sup>
Data Set 1						
1995 Aug 28 .....	49,957.2	15	14	u2uq010t	F814W	(0.053)
1996 Jun 29 .....	50,263.3	7	160	u34d0101t, <sup>b</sup> 2t,ct, <sup>b</sup> dt,nt, <sup>b</sup> ot,yt, <sup>b</sup> zt	F555W	2.023
		7	200	u34d0103t,4t,et,ft,pt,qt,10t,11t	F336W	0.115
		7	100	u34d0105t,6t,gt,ht,rt,st,12t,13t	F439W	0.078
		7	100	u34d0107t,8t,it,jt,tt,ut,14t,15t	F675W	0.949
		7	100	u34d0109t,at,kt,lt,vt,wt,16t,17t	F814W	0.757
		7	100	u34d010bt,mt,xt,18t	F606W	1.531
Data Set 2						
1994 Apr 28 .....	49,470.8	15	14	u2d10206t	F814W	(0.053)
1994 Jul 17 .....	49,550.3	15	14	u2g40409t,at	F814W	(0.053)
1995 Feb 15 .....	49,763.4	15	14	u2g40o09t,at	F814W	(0.053)
1995 Apr 6.....	49,813.7	15	14	u2g40u09t,at	F814W	(0.053)
1997 Jun 26 .....	50,625.6	15	23	u3ak010am,bm	F814W	(0.087)
Data Set 3						
1998 Mar 23.....	50,895.3	15	14	u4ph0101r,a101r,b101r	F814W	(0.053)
		7	14	u4ph0103r,b103r	F814W	(0.106)
		15	80	u4ph0104r,b104r	F439W	0.042 (0.031)
		15	16	u4ph0105r,a103r,b105r	F555W	0.082 (0.101)
1998 Aug 26 .....	51,051.7	15	14	u4ph0201r,br	F814W	(0.053)
		15	100	u4ph0202r,cr	F814W	0.383 (0.379)
		15	80	u4ph0204r,er	F439W	0.042 (0.031)
1998 Aug 26 .....	51,051.7	15	16	u4ph0205r,fr	F555W	0.082 (0.101)
1999 Feb 9.....	51,219.4	15	14	u4ph0301r,br	F814W	(0.053)
		15	100	u4ph0302r,cr	F814W	0.383 (0.379)
		15	80	u4ph0304r,er	F439W	0.042 (0.031)
		15	16	u4ph0305r,fr	F555W	0.082 (0.101)

<sup>a</sup> Values of the background in parentheses are estimates based on a linear extrapolation of exposure time and gain from data set 1 (e.g., for 1994 April 28 in data set 2 we get  $BKG = 0.757 \times 1/2 \times 14/100 = 0.053$  DN).

<sup>b</sup> These F555W exposures were preflashed.

paper. Stetson's use of ground-based observations for the comparison is probably part of the reason for the apparent difference, since this restricts his main sample to brighter stars where the temporal change in CTE is minimal. When he limits his sample to fainter stars he does see an increase in the temporal dependence of CTE loss, although it is still much smaller than reported in the current paper. Another important difference in the two studies is that his measurements use a point-spread function (PSF)-fitting technique while we use simple aperture photometry. By determining the PSF independently for each data set, Stetson's technique may automatically remove some of the effect of degradation in CTE. A direct comparison of PSF-fitting photometry and aperture photometry, using the same data sets and coordinate lists, would help elucidate the reasons for the differences in the two studies.

Another independent study of the temporal dependence was conducted by Sarajedini, Gilliland, & Phillips (1999). The goal of their study was to search for supernovae by

comparing observations of the Hubble Deep Field taken 2 years apart. They find an increase in CTE loss which is in very good agreement with the formulae that will be introduced in § 4. For faint galaxies with  $m_{AB} \approx 24.5$  they find a loss of 0.029 mag from the top to the bottom of the chip, while our formulae give 0.035 mag of loss. For galaxies with  $m_{AB} \approx 26.5$  they find a loss of 0.041 mag while we predict 0.051 mag. Sarajedini et al. (1999) also find no temporal change in the  $X$  (or serial) dependence of the CTE loss. This is consistent with the results from Paper II and the current paper, where the temporal dependence is found to be very weak.

Another important paper relevant to this subject is Casertano & Mutchler (1998), who have studied the nonlinear behavior of the WFPC2 (sometimes called the "long versus short anomaly"). They find that the nonlinearity depends strictly on total counts in the stellar image, and present a simple formula that can be used to correct for the effect, following the correction for CTE loss.

## 2. OBSERVATIONS AND REDUCTIONS

A brief description of the observations and analysis techniques is provided below. For a more detailed description see Paper I.

The set of observations originally used to characterize the spatial and luminosity dependencies were taken on MJD = 50,263 (1996 June 29, hereafter referred to as data set 1). DAOFIND was used to identify the stars, and the PHOT task in the DAOPHOT package was used to perform aperture photometry. Two different aperture sizes were used for the analysis in order to help isolate effects due to differences in the PSF from effects due to CTE or the flat fields. The first aperture employed a 2 pixel radius with a sky value defined by the centroid algorithm in the PHOT task using a 5–10 pixel radius annulus around the star. These aperture sizes were used for both the PC and the WF chips. The second setup used the same sky region but a 5 pixel radius aperture for the stars. Pairs of images were available for the F336W, F439W, F675W, and F814W images. These were combined using GCOMBINE and COSMICRAYS to remove cosmic rays and hot pixels. The images in F555W and F606W were single images with a fair number of cosmic rays. The procedure in these cases, and also for a comparison between individual subexposures for the paired exposures, was to find all objects and then compare them with the F675W master list to filter out cosmic rays.

The same field of view was centered on each of the four chips. The direction of the readout (and hence the orientation of the  $X$ - and  $Y$ -axis on the sky) changes by  $90^\circ$  for each chip. The result is that a star at the top of the chip in WF2 will be on the bottom of the chip when the field of view is centered on the WF4, hence providing an excellent measurement of the differential CTE loss (see Paper I, Fig. 1). The situation is not quite as optimal for comparisons between the other chips, but shifts in the  $Y$ -position are still present; hence it is possible to measure the CTE loss with roughly 50% larger uncertainties.

The data set used to originally characterize the temporal CTE dependence in Paper II (Whitmore 1998, hereafter referred to as data set 2) consists of observations using the F814W filter for eight epochs ranging from 1994 April 28 (i.e., shortly after the cool down from  $T = -77^\circ\text{C}$  to the WFPC2's standard operating temperature of  $T = -88^\circ\text{C}$ ) to 1997 June 26. The F814W filter was employed because it provides the highest signal-to-noise (S/N) determination of CTE for this particular data set, since the stars tend to be red and the background is lower than for the F555W observations. The set of observations in data set 2 used a single pointing; hence, we could not use the method described in the previous paragraph to make differential comparisons. Instead, we used data set 1 to build a database (corrected for CTE based on the formulae in Paper I) and then com-

pared the observations from data set 2 with this “standard field.”

For the current paper we include observations for three new epochs (1998 March, 1998 June, and 1999 February; from proposal 7929), which will be called data set 3. These include observations using the F439W, F555W, and F814W filters and employ the technique of centering the same field on WF2 and WF4. Hence more accurate differential measurements can be made for this data set. Table 1 lists the various observations used in the three data sets.

## 3. RESULTS

In this section we investigate several CTE properties of the WFPC2. We first examine whether CTE loss is the same on all three of the WF chips. We then examine the dependencies on filter, aperture size, previous exposure history, background, and the  $X$ -axis. We conclude with a comparison of CTE on the PC and WF chips.

### 3.1. Comparison of CTE Loss on the Three WF Chips

Figure 1 shows the effect of CTE loss for observations with the F675W filter from Paper I. The throughput ratio is defined as the ratio between measurements of the same star when observed on the various chips. The difference in  $Y$ -positions of a star on the two different chips is plotted along the abscissa of Figure 1.  $Y$ -CTE is defined as the percentage of CTE loss over 800 pixels in the  $Y$ -direction. Only stars with data numbers (DN, also referred to as “counts” in this paper) in the range of 2000–10,000 were included in this particular figure.

The three determinations of the CTE loss in filter F675W in Figure 1 (i.e., the slope in the relation) are in good agreement. A more comprehensive compilation of all six filters, broken into five magnitude bins, results in values of the throughput ratio for WF2 which are  $1.029 \pm 0.047$  larger than for WF3. Comparisons between the other chips yield  $0.965 \pm 0.018$  for WF2 versus WF4, and  $1.006 \pm 0.049$  for WF3 versus WF4, where the mean of the three comparisons has been normalized to 1.00. *We conclude that CTE is identical for each of the three WF chips, with any deviations being less than the statistical noise which is about 5%.*

### 3.2. Observations of CTE Loss with Different Filters

Figure 2 shows the throughput ratios for the F439W filter (largest values of CTE loss from Paper I) and the F555W filter (smallest values of CTE loss), with the different panels showing the data for different brightness ranges. As will be discussed in § 3.5, we believe the difference in CTE properties is simply a function of the background level rather than

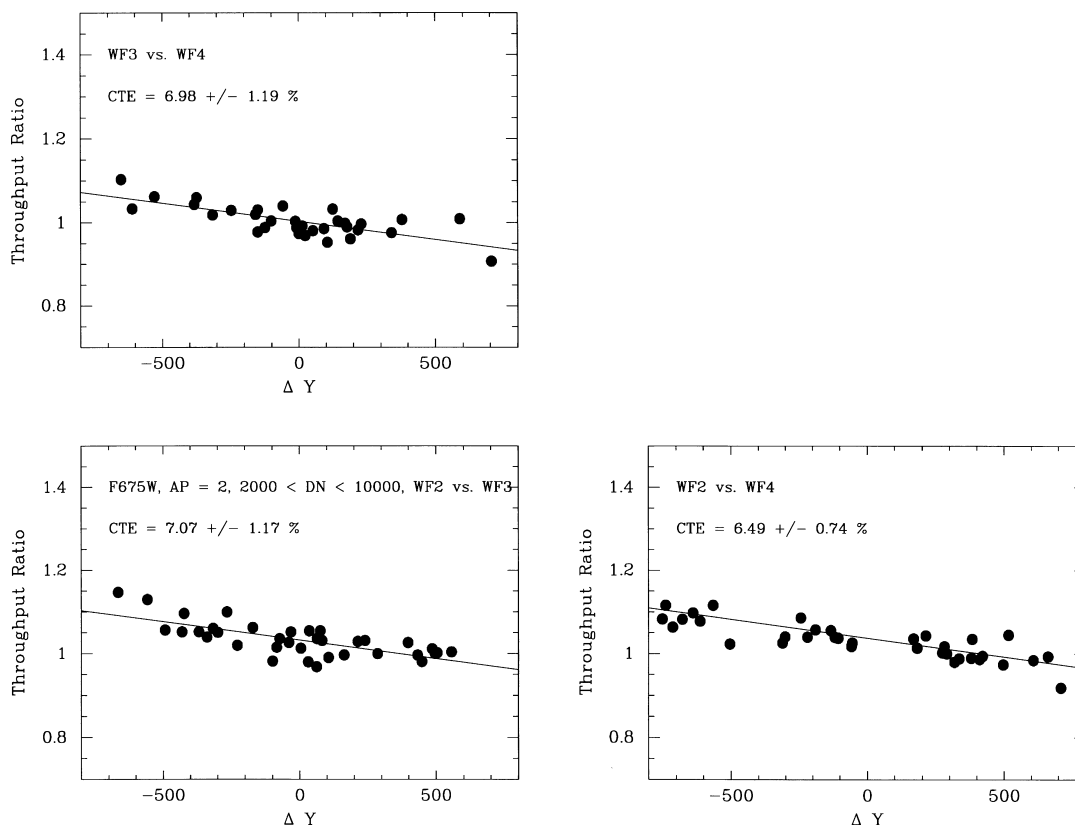


FIG. 1.—Ratio of the difference in the brightness of the same star (i.e., the throughput ratio) as a function of the difference in  $Y$ -position for stars with counts in the range 2000–10,000 DN. The three panels show comparisons between the three WF chips, with the values of  $Y$ -CTE loss in percent over 800 pixels included in each panel.

the result of a wavelength or filter dependence. Only the WF2 versus WF4 observations were used for this particular comparison. The value of CTE loss in percentage over 800 pixels is given in each panel. (See Paper I for the corresponding plots for the other filters.)

Figure 3 shows the measurements from Paper I deemed most reliable (i.e., with uncertainties in the slope less than 4% per 800 pixels) for each of the six filters. The abscissa locations are approximate in Figure 3, adopting mean values of 3500, 1000, 330, 100, and 35 DN for the five bins, and offsetting the longer wavelengths by +0.03. In addition, shorter wavelengths have symbols with fewer vertices (e.g., F336W data points are triangles) while longer wavelengths have more vertices (e.g., F814W data points are circles). The primary result is the dependence on filter (i.e., background level); the more subtle dependence on aperture size will be discussed in § 3.3.

Figure 4 shows a plot of the CTE loss versus the log of the number of counts in the star for the first, second, and combined images. Again, the primary result is the dependence on filter; the small differences between the first and second exposures will be discussed in § 3.4. Our primary conclusions from Figures 3 and 4 are the following:

1. While the “standard” value of 4% (Holtzman et al. 1995) for the CTE ramp is roughly correct for the F555W filter, it is not a good approximation in many other cases.
2. The effect of CTE loss is larger for the faint stars, as has been suggested but not quantified in the past (e.g., Holtzman et al. 1995). Values of CTE loss as high as 15% are present (i.e., the faint stars with the F439W filter) in this data set which was taken in 1996 June.
3. Wavelengths in the midrange (e.g., F555W and F606W) have the lowest CTE loss, with both shorter and longer wavelengths having larger values of CTE loss. This can be seen by the V-shaped distribution of data points in Figure 4 in the cases with full wavelength coverage (i.e., 100 and 330 counts). This is probably because the chips are more efficient at these wavelengths, hence the background is higher. The higher background appears to reduce the CTE loss, as will be discussed in § 3.5.

### 3.3. The Effect of Aperture Size on CTE

The shape of the PSF changes as a function of position on the chip. In addition, if the focus near the top of the chip

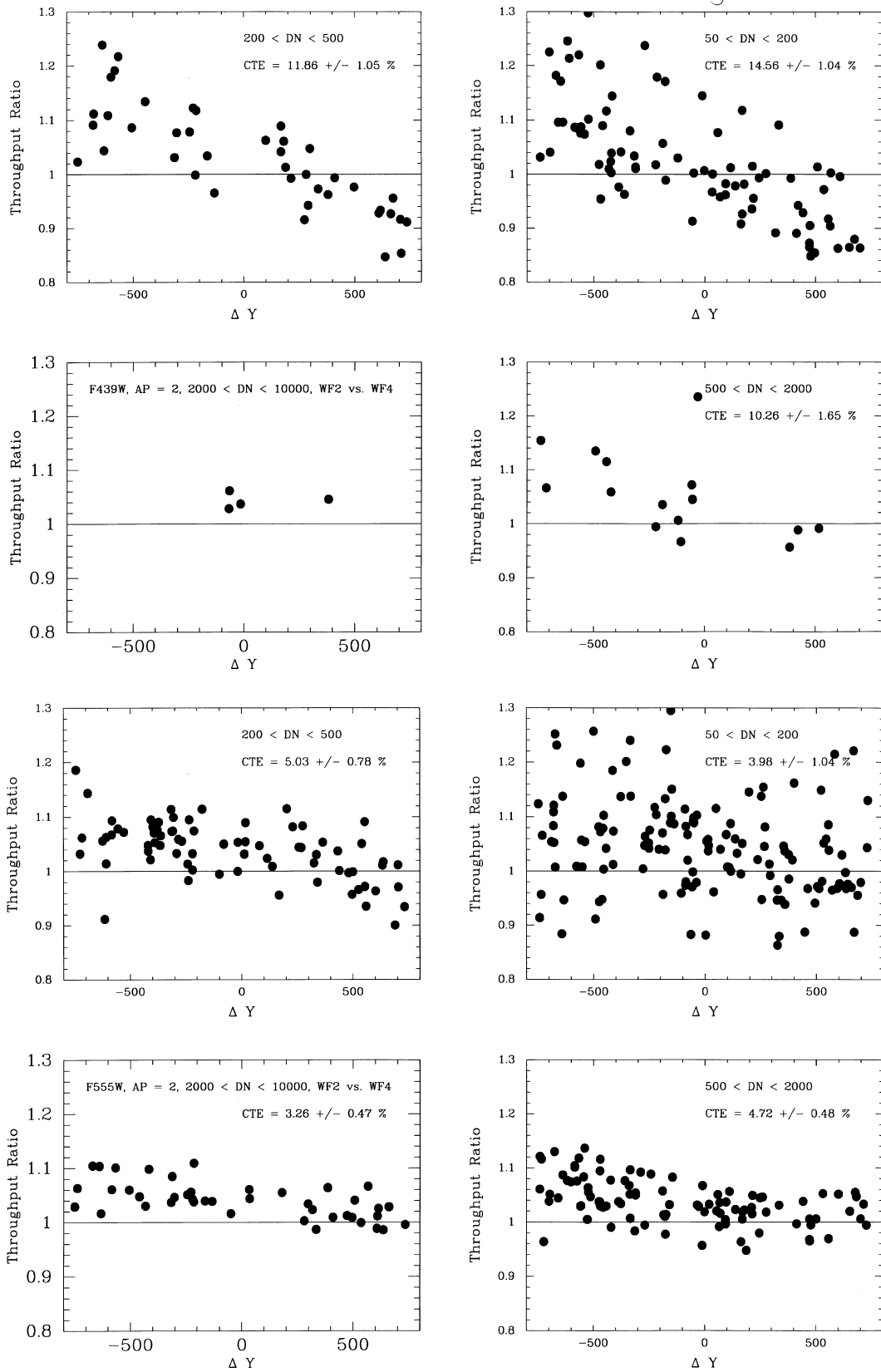


FIG. 2.—Throughput ratio vs.  $\Delta Y$  for the F439W (top four panels) and F555W (bottom four panels) filters. The different panels show the data for WF2 vs. WF4 for different stellar brightnesses (in DN) with the values of Y-CTE loss in percent over 800 pixels included in each panel. From Paper I.

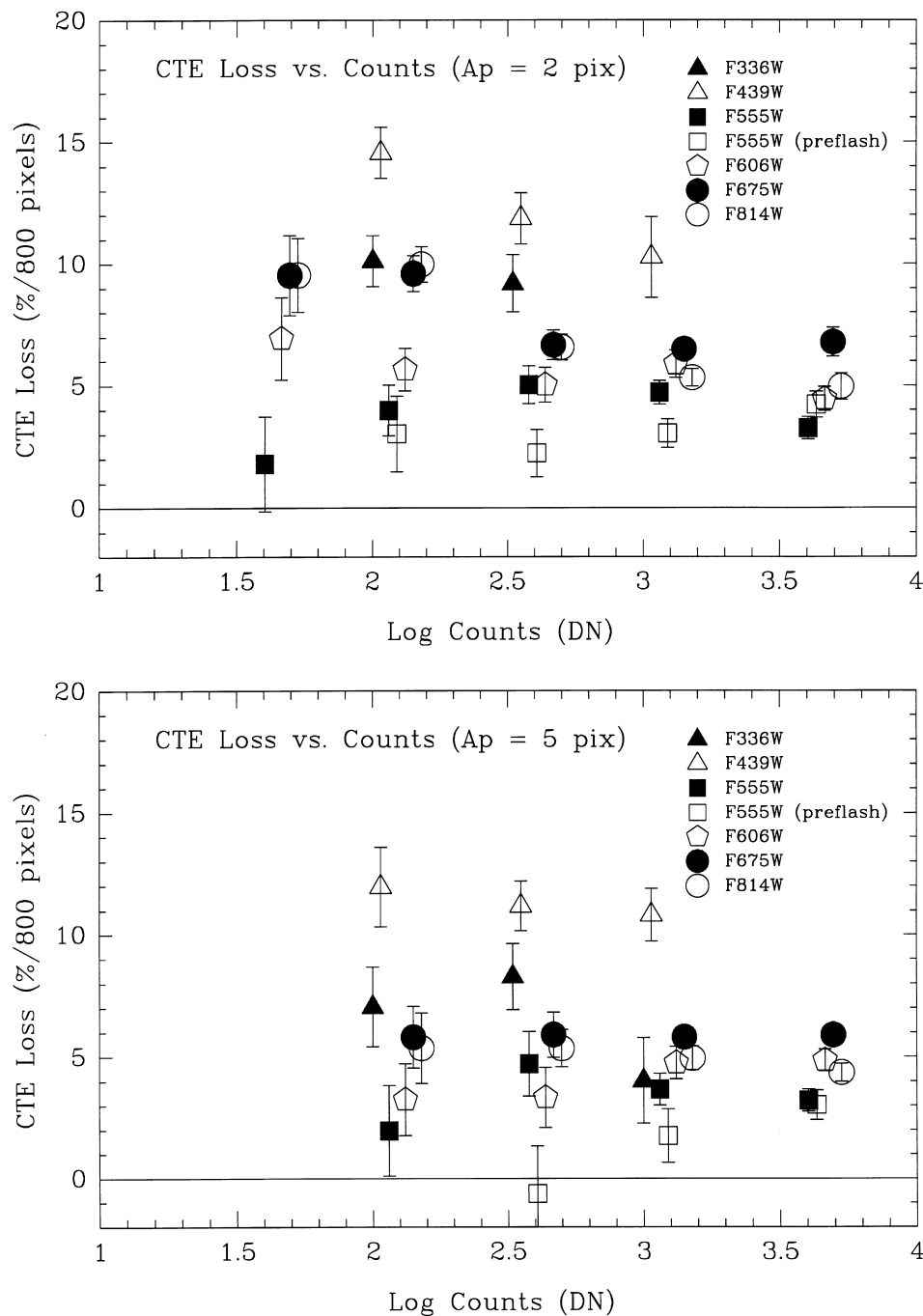


FIG. 3.—Values of  $Y$ -CTE loss in units of percent loss over 800 pixels vs. the brightness of the star in DN. A small horizontal offset has been made as a function of the wavelength in order to reduce overlaps and to show the dependence on wavelength. The top panel used an aperture with a 2 pixel radius, while the bottom panel used an aperture with a 5 pixel radius. From Paper I.

were worse than at the bottom of the chip, small aperture photometry would underestimate the brightness of stars at the top, resulting in a CTE-like effect. One way to check for this is to see if the value of the CTE loss changes when different sized apertures are used.

Figure 3*b* is identical to Figure 3*a* except an aperture with a 5 pixel radius was used. The plots are quite similar,

although there is a small tendency for the fainter stars to have larger values of CTE loss when the 2 pixel aperture is used.

However, we caution the reader from adopting a strategy of using larger apertures in order to reduce the effects of CTE, since in general the uncertainty in the measurements dramatically increases for faint stars. While there is actually

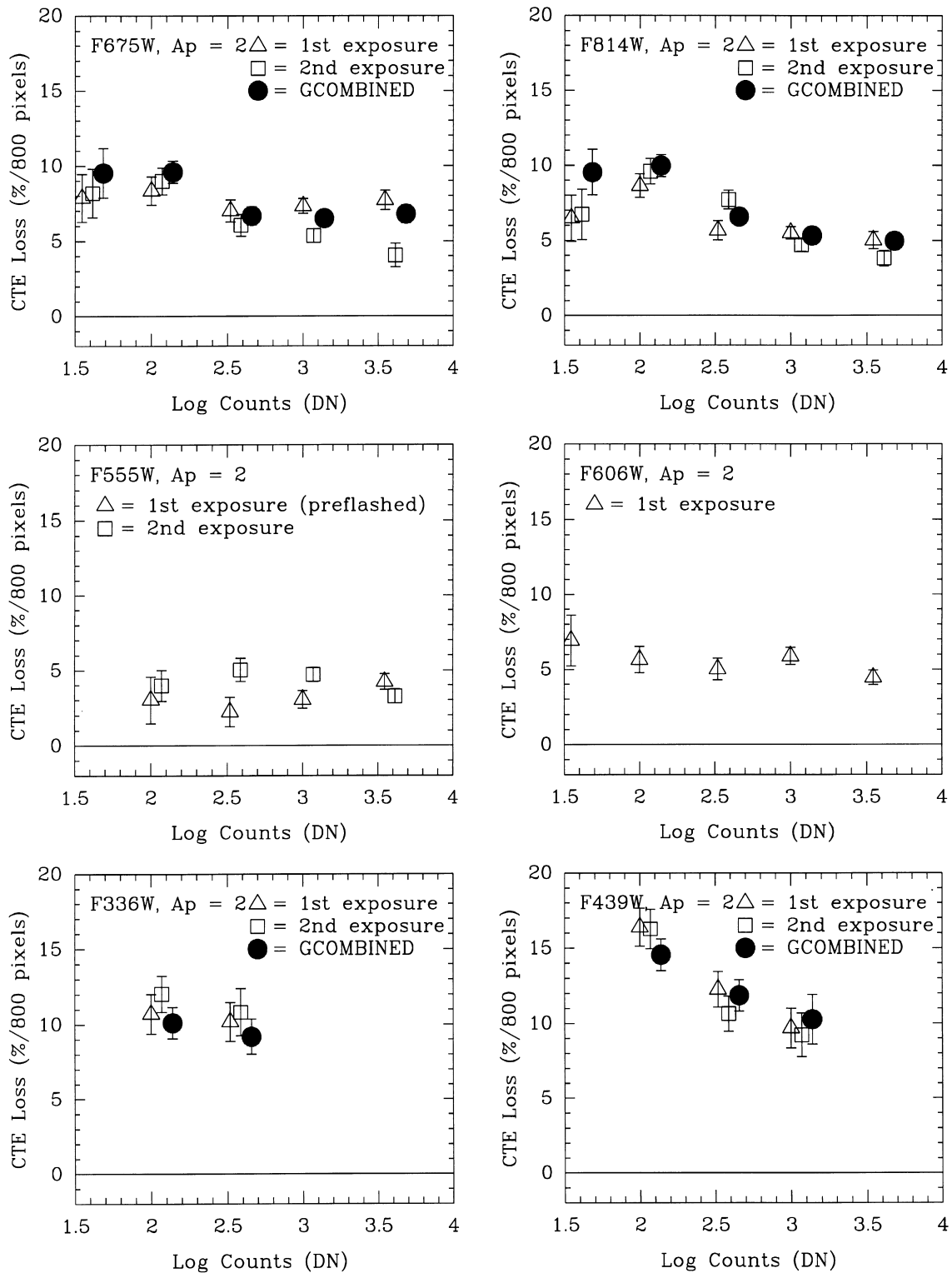


FIG. 4.—Values of Y-CTE loss in units of percent loss over 800 pixels vs. the brightness of the star in DN. The results from the first, second, and GCOMBINED images are included for the 2 pixel aperture measurements. From Paper I.

a slight advantage to using the larger aperture for the very bright stars, or cases where the background is very low (presumably due to the increased number of photons collected compared to the negligible amount of sky), most of the measurements indicate that the uncertainty in the measurement of CTE loss using the smaller aperture is 60% of the uncertainty using the larger aperture (Paper II). Another manifestation of this is that we were able to determine the CTE loss for stars as faint as 35 counts using the 2 pixel aperture, but not the 5 pixel aperture. A spot check comparing results from the 1999 February data set, where CTE loss has increased, gives identical results (within the uncertainties of  $\approx 3\%$ ) when using 2 and 5 pixel radii.

### 3.4. Comparison of First and Second Exposures

A common strategy for minimizing the CTE problem for ground-based CCD detectors is to “preflash” the chip before an exposure, hence filling most of the charge traps before they can affect real exposures. While this does not work very well for the WFPC2 (i.e., the required preflash levels are so high that they make it difficult to detect faint

objects; Ferguson 1996)<sup>5</sup> it raises the question of whether an exposure can be affected by the previous exposure. In particular, is it possible for the first image in a series to act as a preflash for the second image?

Figure 4 shows a comparison of our measurements of CTE for the first, second, and GCOMBINED image. A comparison of the first versus second exposure shows essentially no difference if we include all the data. However, if we look at the five cases with mean counts higher than about 1000 counts (excluding F555W since the first exposure was preflashed), we always find that the value of CTE loss is higher for the first exposure. In the case of F675W the effect is quite large (e.g., 4% and a  $4\sigma$  difference for the brightest stars).

Figure 5 shows the ratio of the measurement in the first and second exposures for the F675W observations. Based on Figure 4 we would expect smaller values of CTE loss for the second exposure; hence we expect the stars to be slightly brighter in the second exposure (e.g., 4% for counts near

<sup>5</sup> H. Ferguson, CTE Calibration, is available on-line at [http://www.stsci.edu/instruments/wfpc2/Wfpc2\\_cte/cte.html](http://www.stsci.edu/instruments/wfpc2/Wfpc2_cte/cte.html).

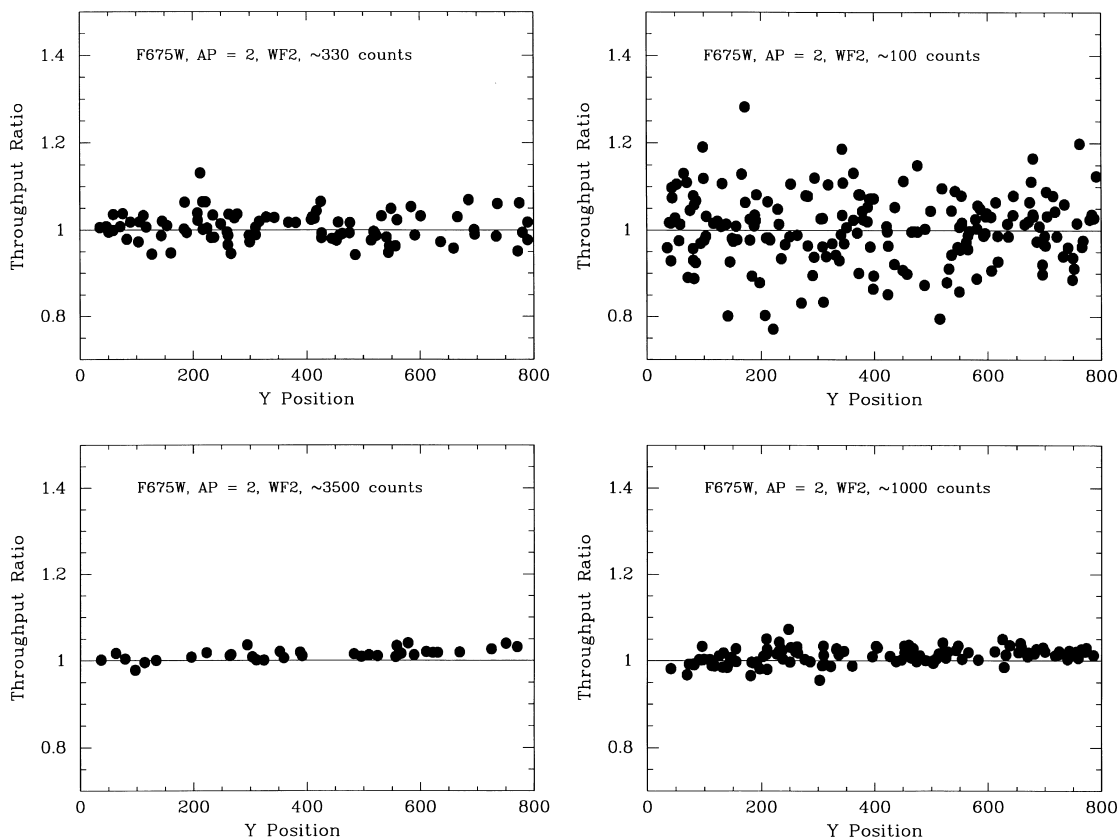


FIG. 5.—Ratio between counts in the second and first exposures vs. the position on the chip for the F675W filter with two exposures, using just the WF2 data. From Paper I.

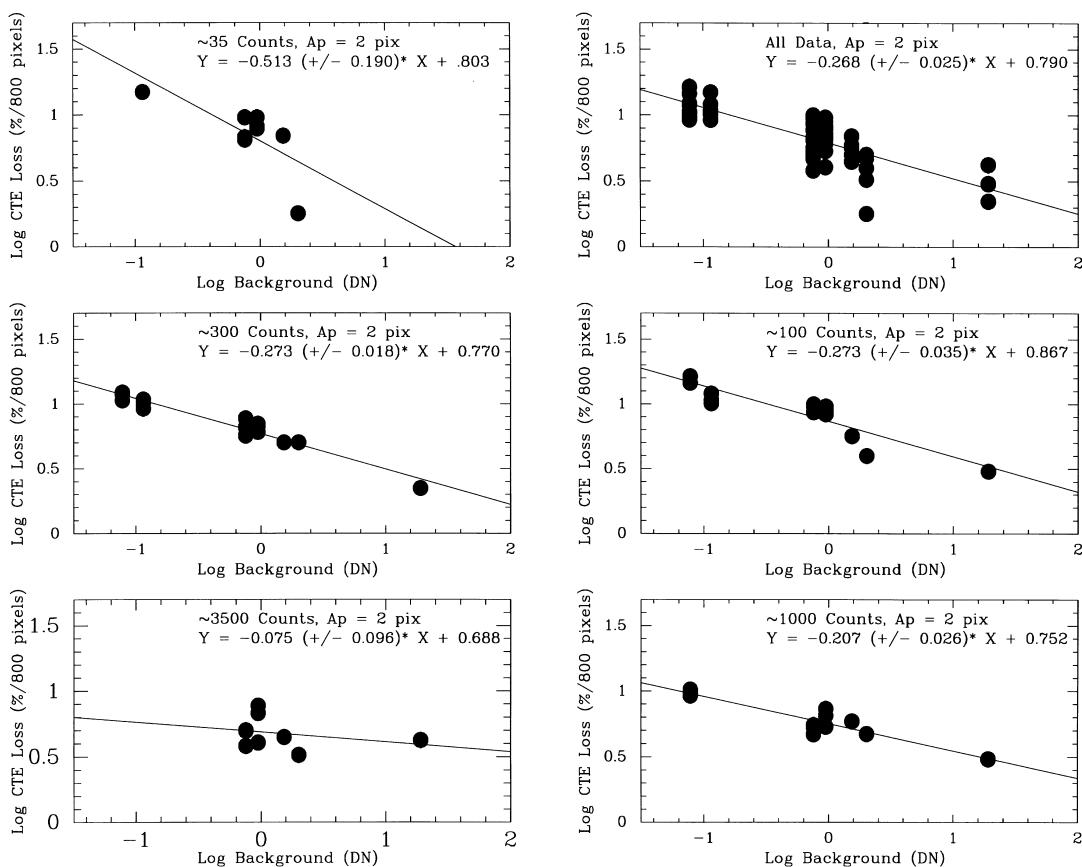


FIG. 6.—Log of Y-CTE loss vs. log of the background. The upper right-hand panel shows the combined results from the other five panels. The low point from the 35 count panel has been excluded from the combined fit. From Paper I.

3500 counts, and 2% for counts near 1000 counts). Figure 5 shows that this is indeed the case. In addition, the difference between the first and second image is a function of Y-position for the F675W filter, as expected.

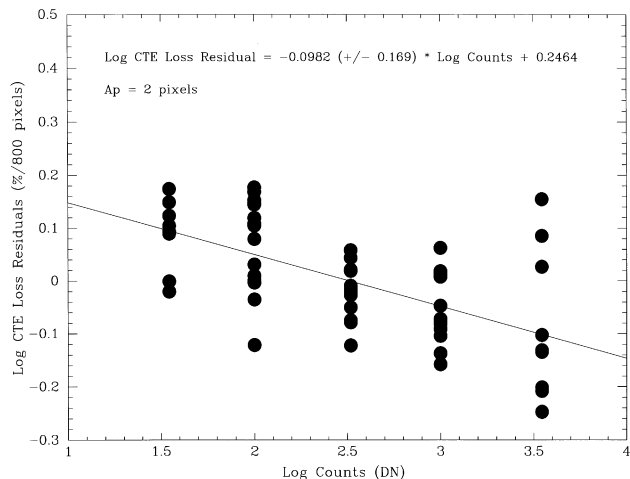


FIG. 7.—Residual from the fit of Y-CTE loss vs. mean background (i.e., the fit in the upper right-hand panel of Fig. 6) vs. the brightness of the star (i.e., log counts). From Paper I.

Hence, there is evidence that the first image acts to preflash the second image in some cases (i.e., primarily the F675W filter), with the value of the CTE loss being reduced and the stars at the top of the chip in the second image being slightly brighter. An obvious question is why the preceding exposure with a different filter does not also have the same effect. Part of the reason might be that the extra time between exposures due to the filter change may reduce the effect, since there is evidence based on residual images that electrons that fill charge traps responsible for reducing CTE loss (e.g., by preflashing) may diffuse out of the traps on timescales of about 20 minutes (Biretta & Mutchler 1997).

However, the fact that the F675W filter shows the largest difference between the first and second exposure may indicate that this preflashing by the previous image actually is important, since the previous observation in this particular case was the F439W image which would not be bright enough to have much effect on the much brighter observations in the F675W filter. This would predict that the F814W filter observations should show little effect, since the preceding images in F675W are brighter and should act as an adequate preflash. This agrees with the observed result. Similarly, this hypothesis may explain why the F336W

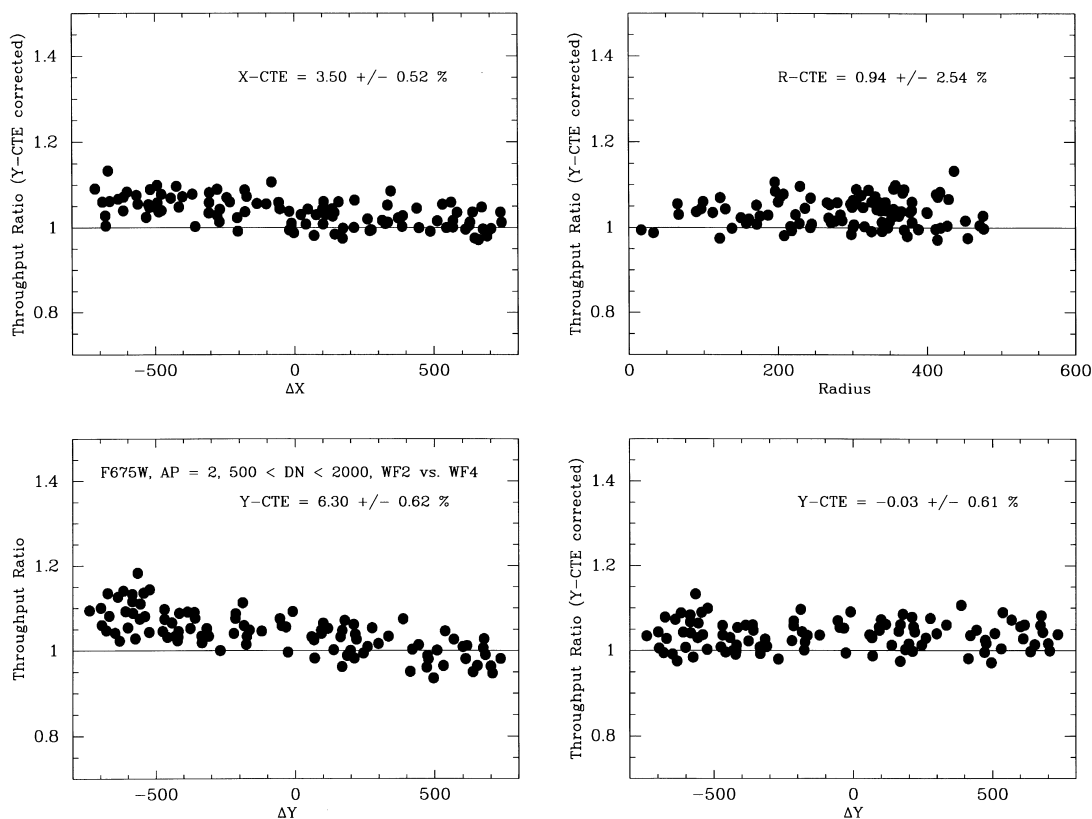


FIG. 8.—Throughput ratio for individual stars with counts in the range 500–2000 counts, using the F675W observations. *Lower left*: The raw result. *Lower right*: Result after the Y-CTE correction has been made. *Upper left*: Shows that there is still some CTE loss along the X-axis. *Upper right*: Shows no significant correlation as a function of the radial distance from the center of the chip, as expected. From Paper I.

observations show a slight inverse relation (i.e., the previous F555W observations acted as a preflash for the first F336W image, but the first F336W image was too weak to preflash the second F336W image) and may be the reason why the F555W images show a slight inverse relation (i.e., the first F555W image was preflashed, which did a better job than relying on the first image to preflash the second image).

Hence, in rough terms it appears that many of the small differences between the first and second exposures seen in Figure 4 can be understood in terms of a consideration of the background level of the previous images.

### 3.5. Dependence of CTE on “Background”

Previous results suggest that CTE loss can be greatly reduced or even eliminated if the “background” is sufficiently high. Holtzman et al. (1995) suggest a ramp of 4% for observations with less than about 30 electrons, 2% for backgrounds of 30–250 electrons, and 0% for higher backgrounds. Ferguson (1996) suggests that a 160 electron preflash reduces the CTE loss to less than 1%. The basic model is that electrons from the background fill the charge traps so that they are not available to trap the electrons in the targets as they are read down the column.

Figure 3 suggests that there may be a correlation between CTE loss and the total number of counts on the chip (i.e., the more efficient filters like F555W and F606W have the lowest values of CTE loss). Figure 6 shows that this is indeed the case, with a good correlation between CTE loss and the log of the mean background in an empty region of the image. CTE loss also depends on the faintness of the star in a systematic way, with fainter stars showing larger values of CTE loss.

Figure 7 shows that the residuals from the correlation shown in the upper right-hand panel of Figure 6 are a function of the brightness of the star. In Paper I this multiple regression was used to establish formulae for removing effects of CTE loss on aperture photometry for data set 1. A slightly different technique will be used in § 4 to derive new formulae which include the temporal dependence.

### 3.6. Evidence for CTE Loss along the X-Axis

One of the surprises in Paper I was the discovery of CTE loss along the X-axis. We will call this X-CTE (or serial CTE). Figure 8 shows that after removing a linear dependence on Y-CTE for the F675W observations, there is still a

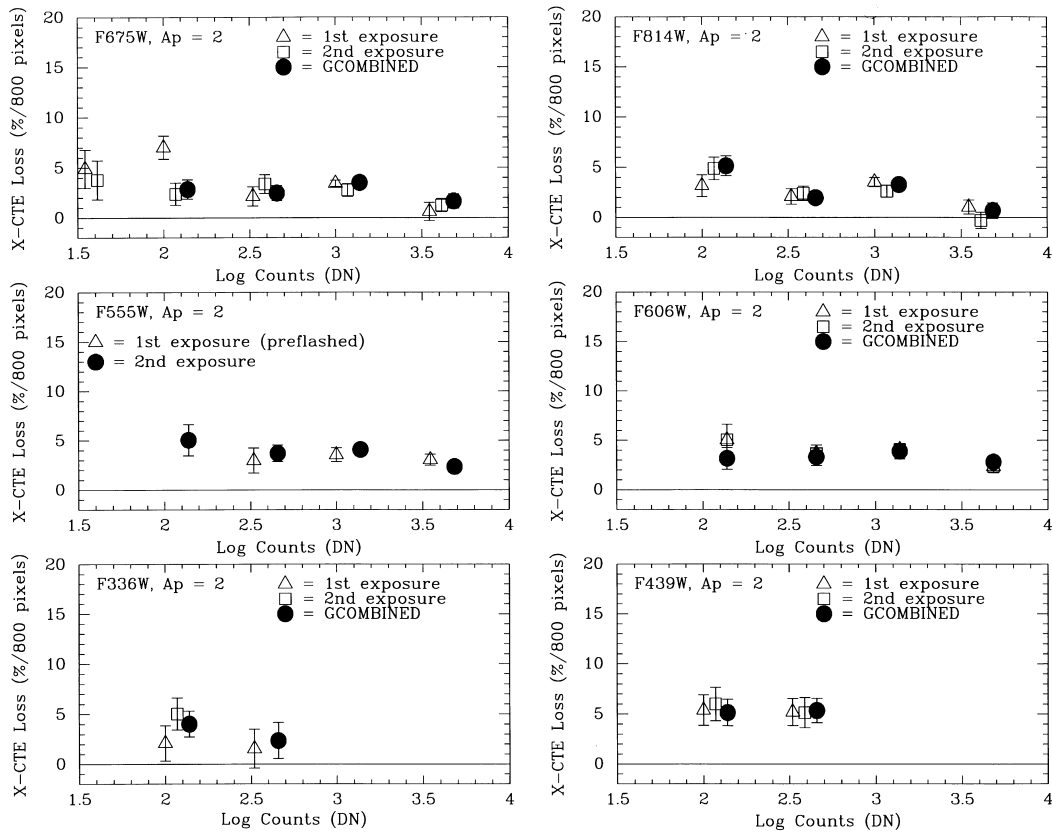


FIG. 9.—X-CTE loss vs. the brightness of the star for all six filters. Note that while there is a dependence on brightness, there is no clear dependence on background level (i.e., F439W and F336W show similar levels of X-CTE as the more efficient filters) or on preflash. From Paper I.

measurable amount of CTE loss on the X-axis, although at a level which is roughly half the normal Y-CTE. A possible explanation is that this is due to CTE loss in the shift register at the bottom of the chip during the readout.

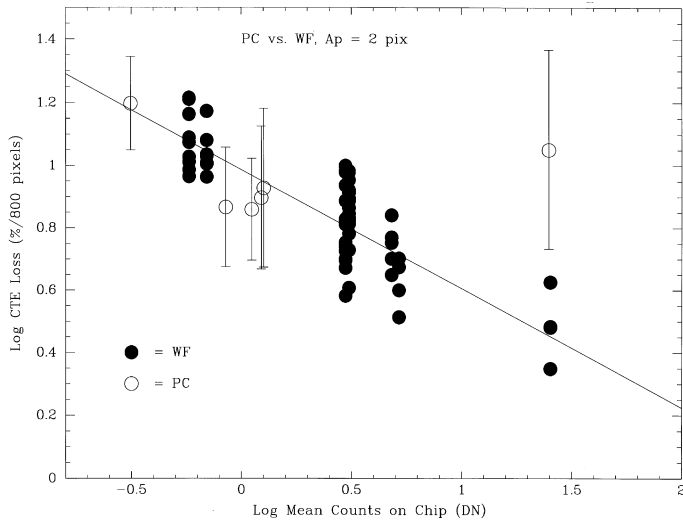


FIG. 10.—Measurements of Y-CTE loss for the PC compared with the WF measurements from the upper right-hand panel of Fig. 6. From Paper I.

Figure 9 shows the values of X-CTE loss for all the filters. The values range from about 1% to 5% for data set 1 which was taken in 1996 June. Note that the preflashed observations of F555W show essentially the same amount of X-CTE loss as the regular F555W observation. Similarly, the amount of X-CTE does not appear to depend on the background level at more than a 2  $\sigma$  level, only on the brightness of the star (see Paper I for further details).

### 3.7. CTE on the Planetary Camera

Measuring the CTE loss on the Planetary Camera (PC) is considerably more difficult than on the WF chips for a number of reasons, primary among them being the fact that there are roughly a factor of 15 fewer stars available for the analysis.

Figure 10 shows that while the measurement uncertainties on the PC are quite large, they are in general agreement with the values from the WF, with the exception of the preflashed measurement of F555W (at log BKG = 1.4) which has the largest uncertainty. Note that this implies CTE values on the PC which are typically a factor of 1.8 higher than on the WF, due to the lower background. *Based on this limited data set, it appears that the same equations can be used to correct for CTE on the PC and the WF chips.*

#### 4. TEMPORAL DEPENDENCE OF CTE ON WFPC2

Figure 11 shows the throughput ratio (in magnitudes) versus  $Y$  as a function of time. The data before 1998 use a comparison between the observations and the standard data set discussed in § 2. This is required due to the fact that observations were only made in a single location. The data taken in 1998 and 1999 employ more accurate (although less numerous since the field for a single chip is used) differential measurements from observations of the same field in WF2 and WF4 (see § 2).

This particular cut is for stars with 50–200 DN within a 2 pixel radius aperture. This corresponds to  $I$  magnitudes in the 18–19 mag range for our 14 s F814W exposures with gain = 15. It is clear that the earlier observations at the bottom of the diagram have much smaller values of CTE

loss than the more recent observations at the top of the diagram.

Figure 12 shows the increase in  $Y$ -CTE as a function of time for four different ranges of target brightness while Figure 13 shows the increase in  $X$ -CTE. For the fainter stars there are clear trends for  $Y$ -CTE. In the case of the 20–50 DN stars and the F814W, 14 s exposures, the CTE loss has increased from 3% to 41%. Table 2 lists the values of  $X$ -CTE and  $Y$ -CTE for Figures 12 and 13.

#### 4.1. Initial Attempts to Develop Correction Formulae

Since  $Y$ -CTE loss appears to increase with time, a first attempt to develop a correction formula was to assume that  $X$ -CTE and  $Y$ -CTE could be expressed as linear functions of time. However, a careful look at the data shows that as

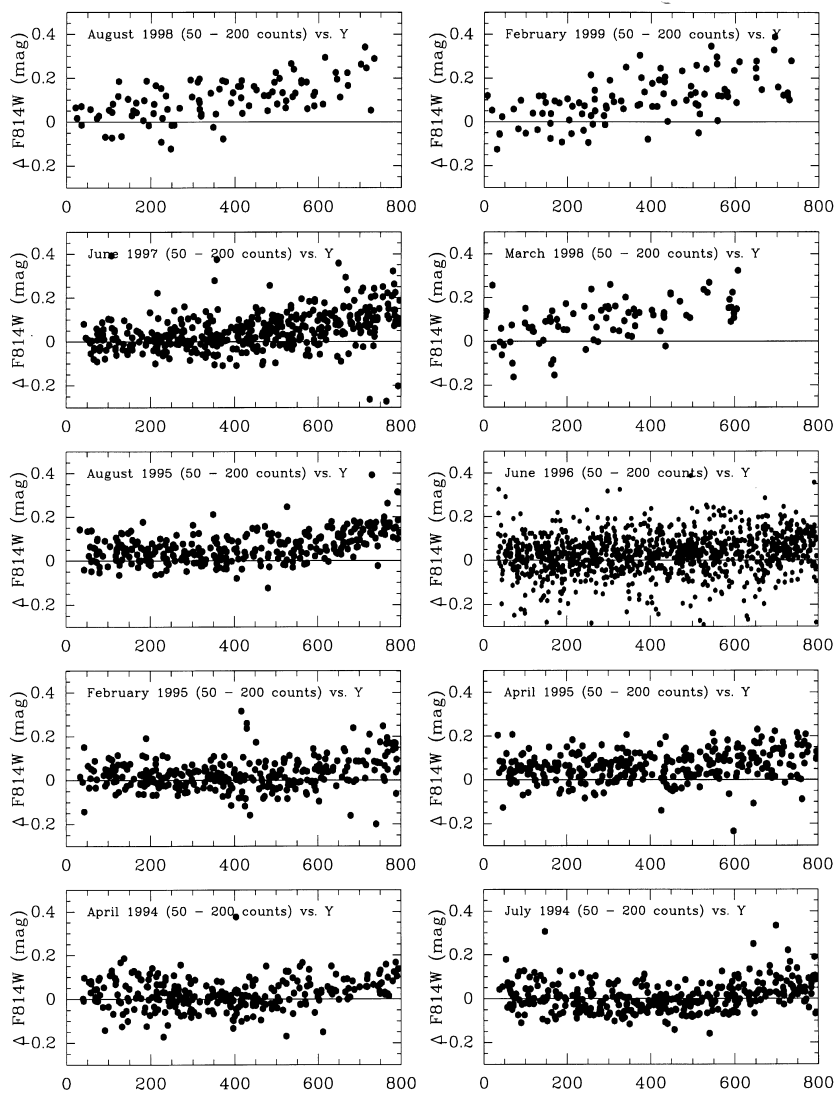


FIG. 11.—Throughput ratio (in mag) in F814W vs.  $Y$  as a function of time

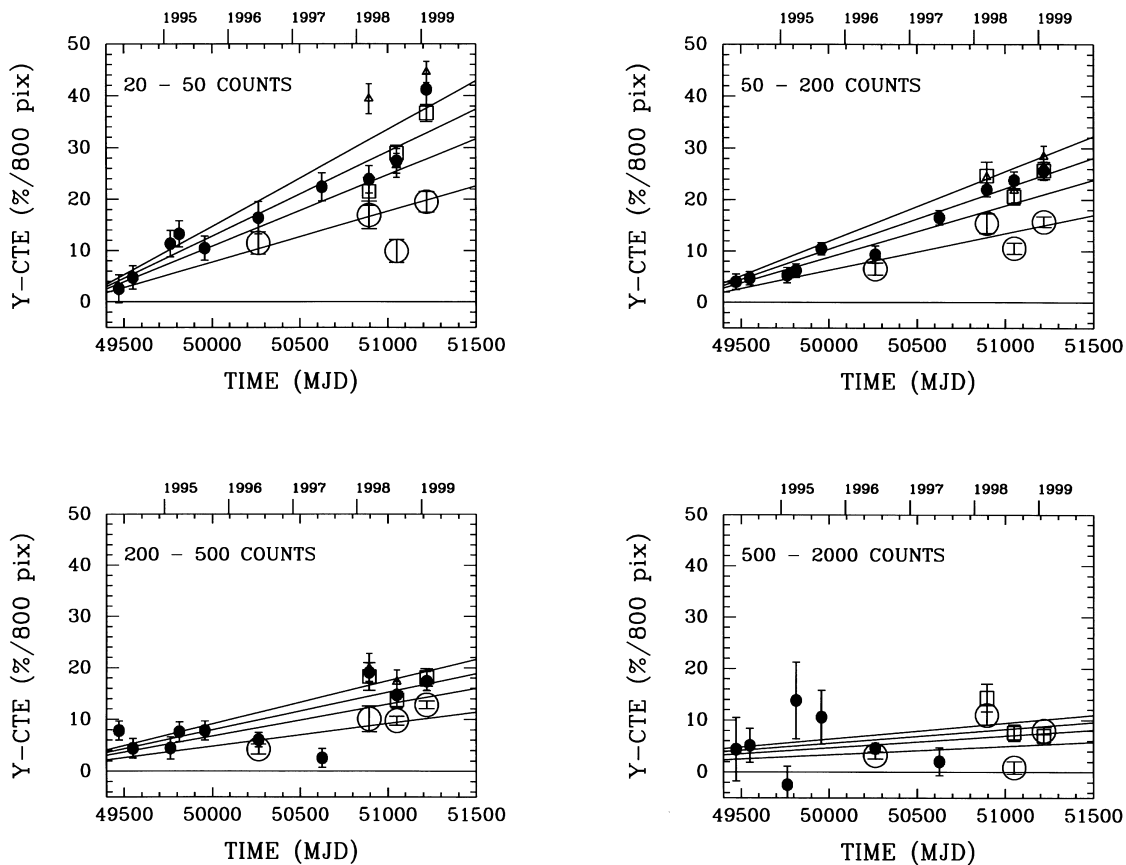


FIG. 12.—Y-CTE loss as a function of time for four different ranges of the target brightness. Triangles are for F439W (BKG = 0.03 DN), squares are for F555W (BKG = 0.05 DN), filled circles are for 14 s exposures with F814W (BKG = 0.10 DN), and open circles are for 100 s exposures with F814W (BKG = 0.38 DN). Smaller symbols are for observations with smaller backgrounds. The lines are for predictions from eq. (1a). See text for details.

the Y-CTE loss increases with time, the difference between bright and faint objects increases as well, as mentioned above. Thus a simple scaling of the Y-CTE effect is insufficient to describe its temporal dependence.

A more general approach is to allow each of the terms that enter in the fit to vary independently with time. So far there is no evidence that the time dependence is anything but linear, so a linear form will suffice as a start. Therefore, we assume as a starting point that X-CTE and Y-CTE are linear functions of  $\log \text{CTS}_{\text{obs}}$  and  $\log \text{BKG}$ , with each of the coefficients also being a linear function of time. The most general such form is

$$\begin{aligned}
 X\text{-CTE} &= A_X + B_X \log \text{CTS}_{\text{obs}} + C_X \log \text{BKG} \\
 &\quad + (D_X + E_X \log \text{CTS}_{\text{obs}} \\
 &\quad + F_X \log \text{BKG})(T - T_0), \\
 Y\text{-CTE} &= A_Y + B_Y \log \text{CTS}_{\text{obs}} + C_Y \log \text{BKG} \\
 &\quad + (D_Y + E_Y \log \text{CTS}_{\text{obs}} \\
 &\quad + F_Y \log \text{BKG})(T - T_0).
 \end{aligned}$$

This expression has 12 unknown coefficients ( $A_X$  through  $F_X$ , and  $A_Y$  through  $F_Y$ ). The optimal values of each coefficient can be found by linear regression methods by fitting to the measurements for each star in all three of the data sets. If we exclude the normalization constants ( $A_X$ ,  $D_X$ ,  $A_Y$ , and  $D_Y$ ), and the coefficients that are not significant at the  $5\sigma$  level, we are left with dependencies on  $\log \text{CTS}_{\text{obs}}$  ( $B_X$  and  $B_Y$ ) at the  $6\sigma$  level, on  $\log \text{BKG}$  for the Y-axis ( $C_Y$ ) at the  $12\sigma$  level, and a temporal increase for the  $\log \text{CTS}_{\text{obs}}$  dependence on the Y-axis ( $E_Y$ ) at the  $21\sigma$  level.

Note that, similar to our results from § 3.6, there does not appear to be a strong dependence of X-CTE on background.

We could proceed at this point to adopt the full 12 parameter fit, or a subset based only on the significant coefficients. However, a careful look at the data showed that the fit is not fully consistent with the model. In general, measurements obtained after 1998 March using the differential technique correlate very well with the fitted solution. However, the fits obtained using the data obtained before 1998, using the less accurate comparison with the standard data set discussed in § 2, are not as good and imply values of

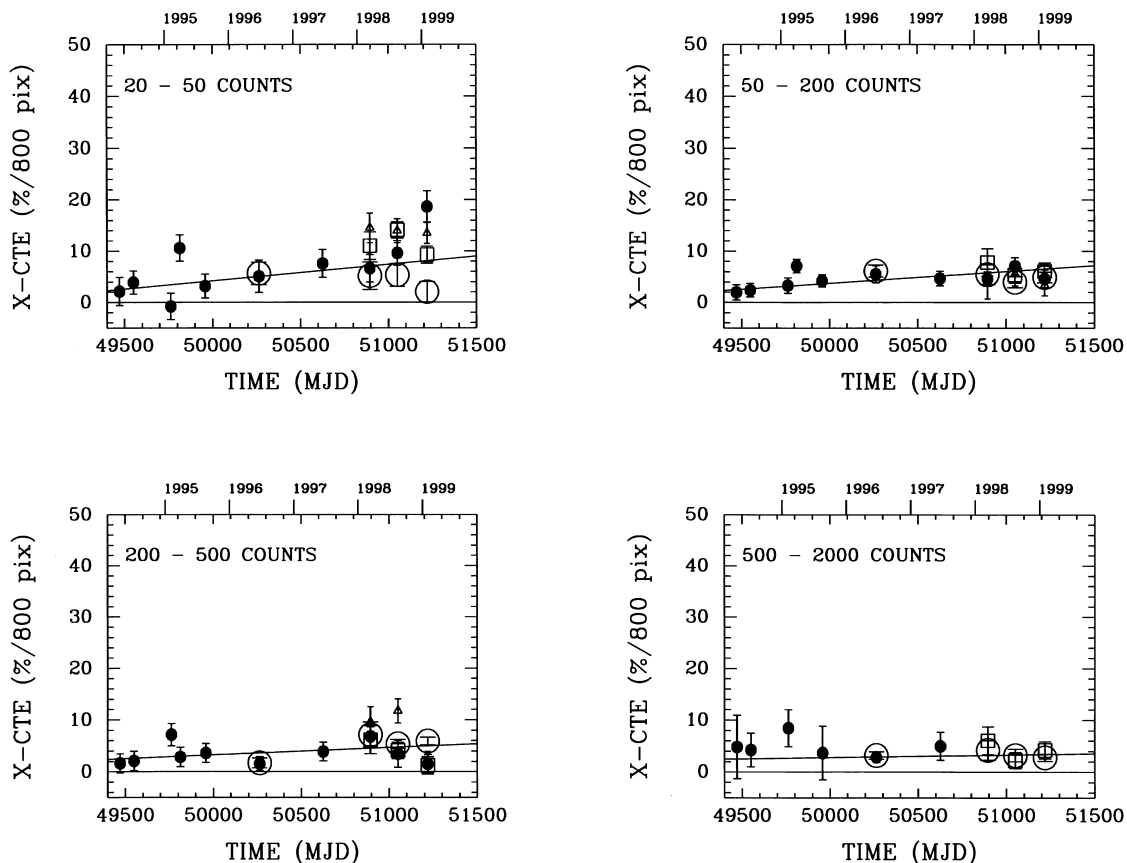


FIG. 13.—Same as Fig. 12 for  $X$ -CTE. The lines are for predictions from eq. (1b).

CTE loss which are not consistent with Figures 12 and 13. Because of these difficulties, a slightly modified procedure has been adopted to determine the final version of the correction formulae.

#### 4.2. Final Correction Formulae

The results from the linear regression discussed in § 4.1 have been used to guide our choice of dependencies to include in the final correction formulae, but the fit is made directly to the data shown in Figures 12 and 13, rather than to the individual measurements for each star.

We first note that for the earliest data set at  $T_0$  (MJD = 49,471) the values of  $X$ -CTE and  $Y$ -CTE are nearly constant, independent of counts. Hence, for the  $Y$ -CTE formula we normalize to the same value at  $T_0$ , use the background dependence based on the results from § 3.5 (see Paper I for details) which include a wider range of backgrounds than used in data sets 2 and 3 (note the lack of a temporal dependence as indicated above), add a  $\log \text{CTS}_{\text{obs}} \times \text{time}$  term based on the data in Figure 12, and normalize to remove the dependence on  $\log \text{CTS}_{\text{obs}}$  for

values greater than 4000 counts (eq. [2a]), as suggested by the data. The final formulae for  $Y$ -CTE are included as equations (1a) and (2a).

A close look at Figure 12 shows that this relatively simple formula fits the data fairly well. The smaller symbols are for the observations with lower background. The lines show the predictions based on equation (1a) for the four backgrounds using the predicted background values from Table 1. The highest lines are for the lowest background with the other lines fanning out in the same sense as the observations with the four different backgrounds.

For  $X$ -CTE we use a single dependence on  $\log \text{CTS}_{\text{obs}} \times \text{time}$ , based on the data in Figure 13. While the 20–50 count panel in Figure 13 hints at a possible dependence on background, the higher S/N results from the 50–200 count and 200–500 count panels do not support this interpretation. The formulae for  $X$ -CTE (eqs. [1b] and [2b]) have again been normalized to remove the dependence on  $\log \text{CTS}_{\text{obs}}$  for values greater than 4000 counts. The final formulae for  $X$ -CTE are included as equations (1b) and (2b), and the fits to the data are included in Figure 13.

We note that these formulae supersede the earlier equations included in Whitmore (1998).

TABLE 2  
VALUES OF X-CTE AND Y-CTE FOR FIGURES 12 AND 13

Date	MJD	Filter	Exposure (s)	Notes	Counts	X-CTE	Uncertainty	Y-CTE	Uncertainty
1994 Apr .....	49,470.80	F814W	14	A	31.6	2.66	3.14	3.20	3.42
					100.0	2.46	1.78	5.01	1.86
					316.0	2.04	2.96	9.77	2.30
					1000.0	6.03	3.91	5.48	7.63
1994 Jul .....	49,550.00	F814W	14	A	31.6	4.85	2.93	5.93	2.84
					100.0	2.98	1.64	5.86	1.64
					316.0	2.61	2.34	5.49	2.35
					1000.0	5.31	3.73	6.41	4.08
1995 Feb .....	49,763.42	F814W	14	A	31.6	-0.99	3.20	14.17	3.21
					100.0	4.11	1.82	6.62	1.87
					316.0	8.94	2.72	5.56	2.70
					1000.0	10.58	3.04	-3.05	4.45
1995 Apr .....	49,813.68	F814W	14	A	31.6	13.25	3.24	16.55	3.19
					100.0	8.87	1.70	7.76	1.65
					316.0	3.55	2.84	9.46	2.38
					1000.0	...	...	17.27	9.25
1995 Aug .....	49,957.25	F814W	14	A	31.6	3.96	3.04	13.07	2.92
					100.0	5.27	1.73	13.09	1.49
					316.0	4.49	2.88	9.77	2.30
					1000.0	4.59	7.01	13.24	6.48
1996 Jun .....	50,263.25	F814W	14	A, I	31.6	6.33	2.61	20.49	3.95
					100.0	6.89	1.36	11.66	2.09
					316.0	1.89	1.08	7.58	1.73
					1000.0	3.59	0.82	5.75	1.26
		F814W	100	A	31.6	7.05	2.91	14.32	2.76
					100.0	7.67	1.51	8.15	1.46
					316.0	2.11	1.20	5.30	1.21
					1000.0	4.00	0.91	4.02	0.88
1997 Jun .....	50,626.00	F814W	14	A, I	31.6	9.45	3.00	27.99	3.42
					100.0	5.84	1.70	20.69	1.78
					316.0	4.86	2.22	3.19	2.26
					1000.0	6.24	2.60	2.55	3.35
1998 Mar .....	50,895.00	F814W	14	D	31.6	8.27	3.64	29.80	3.35
					100.0	5.76	2.39	27.51	1.71
					316.0	8.50	3.92	23.87	2.27
					1000.0	7.61	11.13	17.95	5.15
		F555W	16	D	31.6	13.77	5.44	26.85	5.83
					100.0	9.81	4.06	30.84	3.35
					316.0	7.69	5.86	22.86	3.94
					1000.0	7.61	11.13	17.95	5.15
		F439W	80	D	31.6	18.13	8.47	49.24	8.08
					100.0	4.53	4.83	30.58	3.61
					316.0	12.01	7.45	24.86	4.53
					1000.0	7.61	11.13	17.95	5.15
F814W	100	D	31.6	6.45	3.59	21.12	3.36		
			100.0	6.82	2.39	19.26	2.41		
			316.0	8.90	2.87	12.61	3.10		
			1000.0	5.29	2.65	13.73	2.34		
1998 Aug .....	51,051.00	F814W	14	D	31.6	12.0	4.43	34.27	2.98
					100.0	8.90	3.38	29.75	2.09
					316.0	4.32	4.54	18.38	3.27
					1000.0	5.29	2.65	13.73	2.34
		F555W	16	D	31.6	17.60	5.69	36.10	4.18
					100.0	6.74	3.18	25.81	1.98
					316.0	5.12	4.22	17.23	2.92
					1000.0	2.83	3.64	9.49	3.59
		F439W	80	D	31.6	17.41	5.63	33.20	3.56

TABLE 2—Continued

Date	MJD	Filter	Exposure (s)	Notes	Counts	X-CTE	Uncertainty	Y-CTE	Uncertainty			
1999 Feb.....	51,219.00	F814W	100	D	100.0	6.97	3.86	27.29	2.90			
					316.0	14.65	4.78	21.59	4.39			
					31.6	6.66	2.56	12.37	2.80			
					100.0	4.96	1.58	13.16	1.35			
					316.0	6.69	1.09	12.17	1.07			
					1000.0	4.03	1.67	1.11	1.51			
					31.6	23.31	6.84	51.50	3.81			
					100.0	5.79	3.61	32.04	2.23			
					316.0	1.85	5.05	21.75	2.33			
					31.6	11.56	8.11	45.83	4.08			
		F555W	16	D	100.0	7.59	3.68	32.07	2.07			
					100.0	1.53	4.22	22.66	1.96			
					1000.0	5.29	5.82	8.77	6.37			
					F439W	80	D	31.6	16.86	9.63	55.71	4.85
					100.0			4.21	4.41	35.49	2.56	
		F814W	100	D	316.0	2.32	5.45	22.12	2.46			
					31.6	2.56	2.73	24.39	2.49			
					100.0	6.13	1.83	19.63	1.29			
					316.0	7.37	1.97	16.00	0.92			
					1000.0	3.52	1.18	9.95	0.87			

NOTES.—A: Absolute photometric measurements. See § 2. D: Differential photometric measurements. See § 2. I: Interpolated to 14 s (gain = 7) using CTE equations in Paper I.

For  $CTS_{\text{obs}} < 4000$  DN and  $BKG > 0.1$  DN (see note 2 below),

$$Y\text{-CTE} = 2.3 \times 10^{-0.256 \times \log BKG} \times [1 + 0.245(0.0313 - 0.0087 \log CTS_{\text{obs}}) \times (\text{MJD} - 49,471)], \quad (1a)$$

$$X\text{-CTE} = 2.5 \times [1 + 0.341(0.00720 - 0.0020 \log CTS_{\text{obs}}) \times (\text{MJD} - 49,471)]. \quad (1b)$$

For  $CTS_{\text{obs}} > 4000$  DN and  $BKG > 0.1$  DN (see note 2 below),

$$Y\text{-CTE} = 2.3 \times 10^{-0.256 \times \log BKG}, \quad (2a)$$

$$X\text{-CTE} = 2.5. \quad (2b)$$

For total CTE,

$$CTS_{\text{cor}} = \left[ 1 + \frac{Y\text{-CTE}}{100} \times \frac{Y}{800} + \frac{X\text{-CTE}}{100} \times \frac{X}{800} \right] CTS_{\text{obs}}, \quad (3)$$

where

1.  $CTS_{\text{cor}}$  = number of counts in DN for the star, after CTE correction,
2.  $CTS_{\text{obs}}$  = raw number of counts in DN for the star,
3. Y-CTE = CTE loss in percent over 800 pixels in the Y-direction,
4. X-CTE = CTE loss in percent over 800 pixels in the X-direction,
5.  $X, Y$  =  $X, Y$  positions of the star in pixels, and
6. BKG = mean number of counts in DN for a blank region of the background.

*Note 1.*—These equations are for gain = 7 observations, since this is most commonly used for science observations. For gain = 15, multiply  $CTS_{\text{obs}}$  and BKG by 2 before using equations (1a) and (1b) or equations (2a) and (2b). This has been done to place the lines on Figures 12 and 13.

*Note 2.*—Small uncertainties in the bias level can lead to the measurement of negative values for BKG when the background is very low (i.e.,  $\leq 0.05$  DN). Our recommendation for cases with  $BKG < 0.1$  DN is to linearly scale the value based on observations using the same filters but with longer exposures of the same field, if available. Table 1 shows how this has been done for data sets 2 and 3, based on the longer exposures of data set 1. In cases when longer exposures are not available, and the background is blank sky, approximate background levels can be estimated by scaling the values from Table 1, although changes in zodiacal light and scattered Earth light may limit their accuracy.

Another approach would be to set any measured values of BKG below some threshold (e.g., 0.01 DN) to the threshold value.

## 5. DISCUSSION

While an increase in CTE loss from  $\sim 3\%$  to  $\sim 40\%$  over 5 years for faint stars on faint backgrounds is somewhat alarming, it is important to keep the following in mind:

1. Most science observations are much longer than these calibration exposures (typically 14 s). The result is that the background is much higher, which drastically reduces the amount of CTE loss in most science data.

2. While in the worst cases a single faint star at the top of a chip may suffer 40% CTE loss, the average for a randomly distributed field will only be 20% with a rms scatter of 14%.

3. Using the correction formulae discussed in § 4.2 allows observers to correct their data to a mean accuracy of about 5% or better. Typical observational uncertainties for faint stars, where CTE loss is most critical, are generally much larger than 5%.

A more typical example for a science exposure might be a  $V = 26$  or  $I = 25$  mag star in the center of the chip observed in 1997 using a 1000 s exposure. The formulae predict CTE loss of only 5%–6% in this case. A  $V = 21$  or  $I = 20$  mag star would only suffer  $\approx 2\%$  CTE loss in this example.

It is also important to keep various caveats in mind when using the correction formulae. For example, the formulae were derived using short observations with backgrounds in the range 0.05–2 DN. The agreement of our results with Sarajedini et al. (1999) suggests that extrapolation to backgrounds levels  $\approx 20$  DN are probably reasonable, but beyond that little is currently known. CTE properties for backgrounds fainter than 0.05 DN are especially uncertain since equations (1a) and (2a) blow up at zero (see note 2 after eq. [3] for suggestions on how to handle background levels below 0.1 DN). Similarly, extrapolations for targets fainter than 20 DN are uncertain. However, the large uncertainties introduced by the read noise are generally the limiting factor in these cases. New calibration observations designed to test a wider range of background levels and target brightnesses are currently planned.

Another possible concern is the degree to which the previous image can affect the CTE properties of a given exposure, as discussed in § 3.4. Most of our current tests cover short exposures with low background levels. It is possible that typical science exposures may suffer even larger effects,

since the higher background may serve as a more effective preflash. In addition, the correction formulae were derived using aperture photometry with a radius of 2 pixels. Formulae for other aperture sizes are not yet available (see § 3.3 and Paper I for a discussion of the existing information). Finally, for researchers using PSF-fitting photometry instead of aperture photometry it may be more appropriate to use the results from Stetson (1998). While the correction formulae derived in the Stetson paper are generally in good agreement with our results, there does appear to be an important difference in the temporal dependence which may be due to the method of measurement.

## 6. SUMMARY

Analysis of calibration observations of  $\omega$  Cen lead to the following primary results concerning CTE on the WFPC2.

1. CTE loss is the same on all three WF chips and appears to be the same on the PC, to the degree it can be determined. However, the effect of CTE loss on the PC is generally larger than on the WF due to the lower background.

2. While the main effect is CTE loss along the  $Y$ -axis, there is also a weak CTE problem along the  $X$ -axis (i.e., the stars on the right side of the chip are fainter than those on the left side).

3. Small differences between the first and second exposure in a CR-SPLIT pair can be understood in terms of the previous exposure acting as a preflash for the next exposure.

4. There is a strong time dependence in the amount of CTE loss. In the worst cases (i.e., faint stars on faint backgrounds) CTE loss has increased from about 3% shortly after launch in 1994 to roughly 40% in 1999 February.

5. A set of formulae have been developed to correct for CTE loss when performing stellar aperture photometry with radii of 2 pixels. The formulae have dependencies on the  $X$ - and  $Y$ -position, the brightness of the star, the brightness of the background, and the time of observation.

This paper has benefited from discussions with a large number of people, including John Biretta, Chris Burrows, Harry Ferguson, Andy Fruchter, Ron Gilliland, John MacKenty, Peter Stetson, Massimo Stiavelli, and John Trauger. We especially wish to thank the referee, Jon Holtzman, for many constructive suggestions which lead to improvements in the paper.

REFERENCES

- Biretta, J. S., & Mutchler, M. 1997, Charge Trapping and CTE Residual Images in the WFPC2 CCDs, WFPC2 Instrument Science Report 97-05 (Baltimore: STScI)
- Casertano, S., & Mutchler, M. 1998, The Long vs. Short Anomaly in WFPC2 Images, WFPC2 Instrument Science Report 98-02 (Baltimore: STScI)
- Ferguson, H. 1996, CTE Calibrations (Baltimore: STScI)
- Holtzman, J., & the WFPC2 Team. 1995, PASP, 107, 156
- Janesick, J., Soli, G., Elliot, T., & Collins, S. 1991, Proc. SPIE, 1447, 87
- Sarajedini, V., Gilliland, R. L., & Phillips, M. M. 1999, AJ, submitted
- Stetson, P. B. 1998, PASP, 110, 1448
- Whitmore, B. C. 1998, Time Dependence of the Charge Transfer Efficiency (Baltimore: STScI) (Paper II)
- Whitmore, B. C., & Heyer, I. 1997, New Results on Charge Transfer Efficiency and Constraints on Flat-Field Accuracy, WFPC2 Instrument Science Report 97-08 (Baltimore: STScI) (Paper I)